A Model-based Analysis of Supraspinal Mechanisms of Inter-leg Coordination in Human Gait: Toward Model-informed Robot-assisted Rehabilitation

Vaughn Chambers and Panagiotis Artemiadis*, *IEEE Senior Member*

Abstract— **Stroke survivors are often left suffering from gait instability due to hemiparesis. This gait dysfunction can lead to higher fall rates and an overall decrease in quality of life. Though there are many post-stroke gait rehabilitation methods in use currently, none of them allow patients to regain complete functionality. Interlimb coordination is one of the main mechanisms of walking and is usually overlooked in most post-stroke gait rehabilitation protocols. This work attempts to help further understand the mechanism of interlimb coordination and how the brain is involved in it, studying the contralateral response to unilateral stiffness perturbations. A unique robotic device, the Variable Stiffness Treadmill (VST), is used in conjunction with a pre-established neuromuscular gait model to analyze for the first time the supraspinal control mechanisms involved in inter-leg coordination induced after unilateral perturbations. The attempt to explain the observed kinematic and muscular activation data via the gait model results in the identification of two control variables that seem to play an important role in gait stability and recovery after perturbations: the target angle of attack and target hip to ankle span. This is significant because these two parameters are directly related to longer stride length and larger foot clearance during swing phase. Both variables work toward correcting common issues with hemiparetic gait, such as a shorter stride and toe drag during swing phase of the paretic leg. The results of this work could aid in the design of future model-based stroke rehabilitation methods that would perturb the subject in a systematic way and allow targeted interventions with specific functional outcomes on gait. Additionally, this work—along with future studies—could assist in improving controllers for robust bipedal robots as well as our understanding of how the brain controls balance during perturbed walking.**

I. INTRODUCTION

When a stroke occurs, the brain receives less oxygen due to a blocked or broken blood vessel. This lack of oxygen over time can cause death to brain cells and break neural connections that initiate and control human locomotion. If an individual survives the stroke, there is an estimated 80% chance that they will suffer from some kind of gait dysfunction [1]. One of the most common gait dysfunctions, which is caused by hemiparesis, results in one leg losing sensorimotor functions. This leads to gait asymmetry, most notably in the form of a shorter stride length and less ground clearance of one leg. Not only does this reduce walking speed, which has been shown to correlate with a decreased quality of life, but also leads to unstable gait and a higher

likelihood of falling [2]–[4]. With an estimated 7 million stroke survivors in America today, it is clear that there is a great need for a robust, post-stroke gait rehabilitation method [5].

Since post-stroke gait dysfunction is caused by damage to the brain, the brain must be the focus of the gait rehabilitation protocol. Through the mechanism of neuroplasticity, conscious and repeated training can cause neuronal circuits in the brain to adapt and make structural and functional changes, possibly allowing an individual to relearn actions or motions that were previously disabled due to stroke [6], [7]. Exoskeletons and other devices that assist subjects through the gait motion [8]–[13] have been shown in multiple studies to be no more effective for post-stroke gait rehabilitation than standard treadmill therapy, actually performing worse at times [14], [15]. One factor that these devices neglect to consider is that robust gait requires brain-controlled coordination between the legs [16]–[18]. One school of thought believes that human gait mainly involves two specific mechanisms. First, supraspinal mechanisms initiate gait and adjust to external perturbations. Second, spinal mechanisms send rhythmic patterns to muscles, sustaining unperturbed walking [19]–[21]. Therefore, externally induced perturbations could be used in engaging supraspinal mechanisms for the control of gait, and therefore aid in the brain's neuroplastic recovery.

The Variable Stiffness Treadmill (VST) was developed to allow for repeatable unilateral perturbations that evoke a balance response that requires coordination between limbs [22]. This split-belt treadmill perturbs subjects by decreasing the vertical ground stiffness of a single belt [23], [24]. This unilateral stiffness perturbation simulates taking a step onto a softer surface, such as a yoga mat, grass, or sand. It has been shown in our previous studies that this could be a very useful tool in engaging supraspinal mechanisms involved in gait [17], [18]. Although we have shown evidence that the brain is involved in interlimb coordination after a unilateral stiffness perturbation, it is not yet known what the brain is functionally interested in controlling in this scenario. The brain is presumably balancing the body to keep it upright, but how it is specifically doing so is unknown. Additionally, no gait model has allowed us to replicate walking on the VST, hindering further study of stiffness-perturbed gait.

In this study, human data collected using the VST was used alongside a neuromuscular gait model to understand what specifically is controlled when humans recover from unilateral stiffness perturbations. This model is an estab-

Vaughn Chambers and Panagiotis Artemiadis are with the Mechanical Engineering Department, at the University of Delaware, Newark, DE 19716, USA. vaughn@udel.edu, partem@udel.edu
  *Corresponding author: partem@udel.edu

lished three-dimensional gait model that functions using both supraspinal and spinal control layers [25], [26]. This model was not originally designed to walk on variable stiffness surfaces; therefore, it was adapted by modifying the environment and the supraspinal layer of the model. Altering the environment allowed the model to be put through the same experiment as human subjects. Modifying the supraspinal layer of the model was done to help the model stay balanced for the next step after the perturbation, as it was not originally equipped to withstand such a disturbance. The direct comparison of the collected human response with the simulated (model) response led to the discovery that two supraspinal control variables were essential in balancing the model during and immediately after the perturbation: the target sagittal angle of attack and target hip to ankle span. High level controllers were added to the supraspinal layer to modulate these target variables based on the impulse at heel strike, which is directly related to the ground stiffness of the perturbation. Once the added controllers were tuned properly, the model behaved similarly to human subjects on the VST during the ensuing contralateral step, outputting data with comparable trends. This supports the hypothesis that supraspinal mechanisms may have high-level control functions directly affecting those two variables of human gait. This study, in conjunction with previous works that display the brain's involvement in interlimb coordination [17], [18], may prove useful for model-based gait rehabilitation of stroke survivors with specific functional outcomes.

II. PREVIOUS WORKS

A. Interlimb Coordination

The mechanism of interlimb coordination is vital in post-stroke gait rehabilitation. Humans must constantly adjust to the ever-changing environment around them while walking. Consequently, humans must remain balanced even when changing walking speeds, adapting to different walking surfaces, and avoiding obstacles. This requires a robust coordination between legs [27]. This coordination is essential in stroke rehabilitation as many studies have shown significant brain involvement when steady gait is perturbed unilaterally, resulting in a modulation of interlimb coordination [17], [18], [27], [28]. An additional study shows that during walking, stroke patients were found to have poor functionality in their contralesional limb, not only due to the lesion, but also due to the ipsilesional limb's poor influence [29]. These previous works point toward both the brain's involvement in inter-limb coordination and the effect of interlimb coordination on gait functionality. It is for these reasons that interlimb coordination may play an important role in gait rehabilitation methods, however it is so far largely unexplored.

B. Model-Based Gait Rehabilitation

Model-based approaches in gait rehabilitation offer a myriad of advantages, such as repeatability, patient-specific interventions, predictable outcomes, and accurate tracking of patient's recovery. However, in order to use a neuromuscular model in post-stroke gait rehabilitation, the model must have a few specific qualities. First, the model must simply be proven to work properly. A model would be useless if it was not able to generate human-like locomotion in a variety of circumstances. Second, the model must be complex enough to represent human gait accurately. Assumptions made by an oversimplified model would take the significance out of any conclusions drawn from this model. Finally, the model needs to include the brain, or a simplified version of the supraspinal processes. Without this interaction between the brain, reflexes, and muscles, it would not be possible to gain insight on how to properly provide stroke rehabilitation interventions. It was for this last reason that many candidate models were not seen as a good fit for this study. These models do not rely on the brain to initiate and control locomotion, as gait is generated completely by reflex-based controllers or a predefined set of movements collected from human subjects [30]–[33].

Therefore, the neuromuscular gait model developed by Song et. al. was chosen for this study [25]. This neuromuscular gait model was the only model to meet all three of the above conditions as well as be open-source for academic use. This model is an accurate and complex, three dimensional gait model able to achieve steady locomotion. The model has been shown to output muscle activity and kinematic data similar to that of human subjects in a variety of steady-state situations as well as in a few disturbance experiments [25], [26]. In one of these experiments, the model was unilaterally perturbed by shifting the ground under one of its feet during stance phase, simulating slipping. The model's behavior compared extremely well with human subject data from the same test. Previous studies such as this prove the validity of the model and suggest it is a good fit for our study. The model consists of a trunk, thighs, shanks, and feet. Revolute joints make up the hips, knees, and ankles, with 2 degrees of freedom (DoF) at each hip, 1 Dof at each knee, and 1 Dof at each ankle. The model interacts with the ground through 4 contact points on each foot. Gait is goal-driven through the following 3 tasks, in order of decreasing importance: stay upright, achieve steady gait, and minimize energy usage. The version of the model used in this study is calibrated (or optimized) to walk on flat ground, in a straight line, at an average walking speed. Locomotion is controlled at its highest level by a supraspinal layer that sets desired foot placement, foot clearance, and trunk angle, and decides which leg will take the next step. The spinal layer then works based on the information passed along from the supraspinal layer, and considers 10 modules during stance or swing to achieve what the supraspinal layer instructs. Next, the spinal layer sends specific inputs to each of the 22 Hill-type muscle tendon units (MTU). The MTUs put the body in motion, where it then interacts with the environment and attempts to walk and remain upright [25]. The complexity, accuracy, and presence of a supraspinal layer make this model a great fit for this study, which aims at investigating supraspinal processes in complex environments.

C. Variable Stiffness Treadmill (VST)

The VST is a unique tool for evoking brain involvement in gait. The VST is able to perturb the subject through unilateral stiffness perturbations at any point in the stance phase and for any amount of time [22]–[24]. When a stiffness perturbation occurs, one side of the treadmill lowers its stiffness, simulating walking on a soft surface. Previous experiments with the VST have suggested that this unilateral stiffness perturbation results in brain involvement that controls interlimb coordination. Specifically, after a unilateral stiffness perturbation, a response on the contralateral (unperturbed) leg is not seen for 150ms [18]. This latency of >150ms suggests a transcortical reflex mechanism [34]. Another VST experiment captures electroencephalographic (EEG) data of the subject during gait perturbations. In this experiment, the subject's left leg is perturbed, but significant changes are seen on the left side of the brain, which is responsible for controlling the right side of the body [17]. These past experiments show evidence of the brain's involvement in controlling the contralateral side of the body during a unilateral stiffness perturbation.

III. METHODS

A. Experimental Procedure

In an effort to investigate mechanisms of interlimb coordination during human gait, an experiment was conducted using five healthy subjects (age 25 ± 5.4 years, weight 845 ± 156 N) on the Variable Stiffness Treadmill (VST). For the duration of this experiment, the subjects were supported by a body weight support harness, offloading 30% of their total weight. Note that the body weight support was for safety only and has been shown to not influence muscle activity at a value of 30% [35]. While walking on the VST, the subjects were unilaterally perturbed (on their left side) by a lowering of ground stiffness. These decreased stiffness perturbations began at about 130ms after left heel strike and lasted for the rest of the left stance phase. The decreased stiffness perturbations had values of 100kN/m, 50kN/m and 10kN/m, where 1MN/m was assumed rigid. The right side of the treadmill was to remain at 1MN/m, or rigid, for the entirety of the experiment. Since we are interested in the mechanisms of interlimb coordination, only the contralateral (right) leg was observed during this study by recording muscle activity and kinematic data. This data consisted of tibialis anterior (TA) activity, soleus activity, hip flexion-extension angle, knee flexion-extension angle, and ankle dorsiplantar flexion angle. It should be noted that a random number of unperturbed steps, ranging from 3 to 7, were left in between successive perturbations to allow the subject to regain their balance and not anticipate the next stiffness perturbation. Each subject withstood an average of 17 ± 2.3 perturbations at each stiffness level [17]. These experimental protocols are approved by the University of Delaware Institutional Review Board (IRB ID#: 1544521-1) and subjects gave informed consent.

B. Modeling

A neuromuscular gait model was then put through the same conditions as in the human experiment. This model has proven to be valid in a variety of unperturbed circumstances and a few perturbed circumstances, but was not initially equipped to allow for walking on a variable stiffness surface [25], [26]. Therefore, the model needed to be adapted to simulate the unilateral variable stiffness environment, while allowing the introduction of a set of supraspinal control circuits necessary to remain balanced through such a perturbation. The added supraspinal controller modulates the target angle of attack (AoA) and target hip to ankle span (H2AS) after a unilateral stiffness perturbation, for the next swing phase of the contralateral leg. These variables are explained in detail below. After the model's environment was updated to allow for a variable stiffness ground and the supraspinal controller was added, we were able to begin tuning this controller to make the model behave more like the subjects in the human experiment. We were able to measure how well the model's response replicated the human response by comparing the TA activity, soleus activity, hip flexion-extension angle, knee flexion-extension angle, and dorsiplantar flexion ankle angle for the contralateral swing phase following the onset of the perturbation. The high-level controller was tuned until the model's response best mimicked the human response.

C. Model Adaptation

In this study, we wanted to examine interlimb coordination after a unilateral stiffness perturbation, so we altered the model to allow for this. The model interacts with the ground by using four contact points on each foot. For each of the contact points of the left foot, which is on the perturbed side, the stiffness of the interaction between the contact point and the ground was changed from a constant value to a variable controlled using a gain and a switch. This allowed both the magnitude and timing of the stiffness perturbation to be easily controlled.

We tested the model immediately after making these changes, and unsurprisingly, the model was not able to stay balanced after the stiffness perturbation. After the low stiffness perturbation on the left side, the right foot would demonstrate toe drag and the model would fall forward immediately (as depicted in Fig. 1). We concluded that the model was not currently set up for walking on soft surfaces.

In an attempt to balance the model after the perturbation, we decided to alter two target variables in the supraspinal control layer of the model. These two variables, the only two control variables for this study, were target angle of attack (AoA) and target hip to ankle span (H2AS)[1]. The AoA is the angle made between the ground and the straight line connecting the hip and ankle of the swing leg. The target AoA is the desired angle to be made upon heel strike.

---

[1]In previous versions of the model by Song et al., target AoA & H2AS are α_{tgt} & l_{clr}, respectively. These variable names were changed for this work to improve clarity.
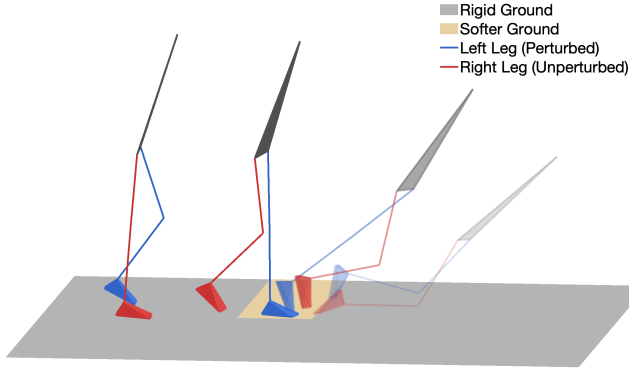
Fig. 1. Unaltered neuromuscular gait model cannot remain balanced after a 10kN/m unilateral (left leg) stiffness perturbation.

The angle of attack determines both how far to flex the hip during swing and the overall stride length, with a smaller target angle leading to a longer stride (illustrated in Fig. 2a). The H2AS is the straight-line (Euclidean) distance between the hip and ankle of the swing leg. The target H2AS is the desired minimum distance to be achieved during swing phase to avoid toe drag. A lower target H2AS would result in the foot being brought higher off the ground during swing, shortening the distance between the hip and ankle (illustrated in Fig. 2b) [25]. These parameters were chosen because the combination of these two variables essentially plan out the model's entire swing phase. In this model, as well as in previous iterations of this model, swing is achieved through three main tasks [25], [30], [36]. First, the knee must flex after toe off to achieve the target H2AS to avoid toe drag. Next, the hip must flex to a desired value to place the foot above a desired location that meets the target AoA. Finally, the knee must extend to reach the ground and achieve heel strike [37]. Together, the target AoA and target H2AS were proposed to be sufficient in balancing the model as they correct the issues of toe drag and falling forward that the model originally experienced under stiffness perturbations.

Now that we had the idea of changing the target AoA and target H2AS, we needed to create circuitry in the model to allow it to recognize a lower stiffness and adapt. To achieve this, a mechanism was added that measured the impulse felt J, during the initiation of heel strike, as shown below:

$$ J = \int_0^\tau F dt \tag{1} $$

where $\tau = 0.092s$, and F is the measured vertical force as the leg touches the floor. This specific τ value was selected because it allowed the model to gather enough data without adding large delays into the system. The impulse felt on that step was then compared to the impulse felt when walking on a rigid surface (J_o), which can be thought of as what the model expected to feel. Based on the error between these values ($\Delta J = J - J_o$), a value is calculated that acts as a gain that scales the target AoA and target H2AS for the ensuing contralateral swing phase (see block diagram in Fig. 3). Both of these values were decreased as the ground stiffness got softer, making the model take a bigger step and

lift the leg higher during the right leg swing phase after a left leg perturbation.

It should be noted that, for the sake of simplicity, the target H2AS of the model only affects the angle of the knee. To properly avoid toe drag, the ankle angle should be affected as well. To account for this, an additional low-level controller was appended that adds extra stimulation to the tibialis anterior proportional to the change in H2AS. This pattern of scaling dorsiflexion with H2AS was missing from the model and affected our study. Again this was done to help the model more closely resemble human gait and better avoid toe drag. This low-level controller simply adds an extra gain into the controller that stimulates the tibialis anterior muscle in the model. The equation of the controller was empirically found to be $T_n = T_o + 3\Delta h$, where T_n is the new TA gain, T_o is the original TA gain, and Δh is the change in the H2AS. There are a few studies that suggest the TA is controlled in part by supraspinal mechanisms [38], [39]. But since this controller is not the focus of this study, and was simply a small improvement to the model, it will not be discussed any more for the remainder of the paper. The rest of this paper will focus on the high-level controller discussed more in the paragraph below.

D. High-Level Controller Development

To properly formulate and tune the aforementioned supraspinal controller, the best measure of success was to consider how well the model displayed human-like behavior (i.e. how well the model simulated the experimental results). While we could simply look at how long the model stayed balanced after the perturbation, we do not believe this alone would have been a sufficient gauge. This is because we were only affecting the behavior of the right step directly after the perturbation, so the model would later fall after a few more steps no matter how well we tuned the high-level controller.
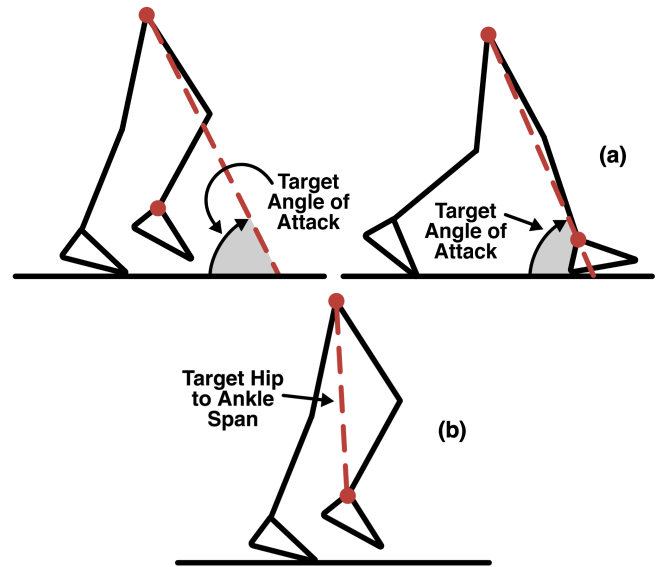

Fig. 2. (a) Target angle of attack being approached (left) and achieved (right) during swing phase. (b) Target hip to ankle span during swing phase being achieved to avoid toe drag.
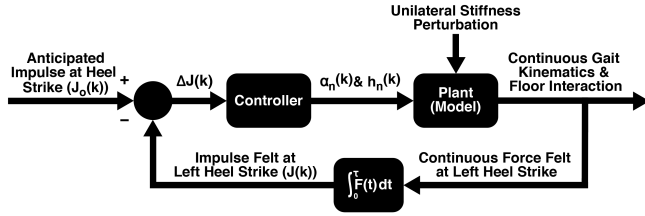
Fig. 3. Block diagram of added high-level controller that alters target angle of attack and hip to ankle span of right leg based off impulse felt at left heel strike. Note: (t) indicates continuous time variables, while (k) indicates discrete time variables.

So, the best way we found to measure the validity of the controller was to compare muscle activity and kinematic data of the right step following the left side perturbation for the model with real human data from the experiment on the VST. The main comparison was with the experimental results shown in Fig. 4a, displaying tibialis anterior and soleus muscle activity, as well as hip, knee and ankle kinematics in the sagittal plane. The data from the model was compared to these graphs based not only on values, but also on overall trends.

In order to find an equation for the high-level controller, we empirically tested different AoA and H2AS values and compared the muscle activation (TA, SOL) and kinematics (hip, knee, ankle) of the contralateral (unperturbed) leg to the experimentally collected human data. The criteria used when assessing the model's data were as follows. First, there needed to be separation between trials. The model should react to different perturbation levels in different ways. Second, as the different trials separate from each other, they should deviate from the rigid trial in order of decreasing stiffness. For example, the model's reaction to the 10kN/m trial should differ from the rigid trial more than the 100kN/m. Third, the overall shape of each trial should be similar to the rigid trial. There should only be slight changes in magnitude and not any extreme outliers. Fourth, the correlation coefficient was computed between the simulated model data and the human data. A coefficient closer to $+1$ indicates a better match. This was found to be effective only to a degree due to the difference in rigid (or baseline) trials. In other words, without a perturbation, the muscle activity and kinematic data for the model and human are not exactly the same in profile and magnitude. This led to the idea of finding the correlation coefficient between the human and model data after the baseline rigid trial had been subtracted. This method then compares the change in response from rigid walking, which we thought was appropriate for this study. Again, a coefficient closer to $+1$ indicates a better match.

After using these methods to carefully compare the human and model data among all three perturbation stiffness levels (100kN/m, 50kN/m, and 10kN/m), we formulated the following equations (2). These equations define the new target AoA (α_n) and H2AS (h_n) as functions of the previously calculated corresponding values, (α) and (h), respectively. Note that (α) and (h) are the target values calculated by the model for rigid ground walking.

$$\alpha_n = f\left(\Delta J, m\right)\alpha, \qquad h_n = g\left(\Delta J, m\right)h \qquad (2)$$

where f and g are functions of the difference/error in the impulse felt when walking on a rigid and a compliant surface (shown in Fig. 3), as well as the mass (m) of the subject. These equations therefore account for an adjustment of the corresponding control variables, as α and h are calculated for rigid walking surfaces. After comparing simulated and actual data, the following functions were identified.

$$f\left(\Delta J, m\right) = \frac{a_1\Delta J}{m} + b_1, \quad g\left(\Delta J, m\right) = \frac{a_2\Delta J}{m} + b_2 \quad (3)$$

where $a = a_1 = a_2 = -0.32\frac{Kg}{Ns}$, and $b = b_1 = b_2 = 1$, i.e. the two function f and g ended up being equal ($f = g = G$). Note that G will be used to represent the gain used to modulate the AoA and H2AS for the remainder of the paper. The parameters for these functions as well as all following functions were determined through the method of least squares. For the different stiffness levels, the change in impulse (ΔJ) was found from the response of the model, while the AoA and H2AS gain (G) was found empirically to best fit human data. Now that data points were found (G vs. ΔJ), an equation was fit to that data with an R^2 value of 0.96.

To summarize, here is an example of how the above high-level controller works. When the model steps on a softer surface, the impulse felt will be less than expected, resulting in a positive ΔJ value. This value is the input to (3), which outputs the gain to be multiplied by the original AoA and H2AS to obtain the new values. These new values will be less than the original, resulting in a longer stride and more foot clearance, respectively.

IV. RESULTS

A. Kinematics & Muscle Activity

The results of this study show that by altering the target angle of attack (AoA), target hip to ankle span (H2AS) and the activation of the tibialis anterior in relation to the H2AS, we were able to produce muscle activity and kinematic data from the model that agrees with the human experimental data. This similar output can be seen by comparing the human data (Fig. 4a) and the final model data (Fig. 4c). For comparison, the model output without the developed high-level controller is shown in Fig. 4b.

Large differences can be seen when comparing the human response of the unperturbed leg (Fig. 4a) to the initial model response of the unperturbed leg (Fig. 4b). As this is data from the model pre-modification, the model is not sufficiently changing its gait for different perturbation levels. A general trend with this data is that the rigid, 100kN/m, and 50kN/m trials all generate about the same response, while the response to the 10kN/m trial was extremely different. This is not a human-like response and is due to the model walking nearly the same way no matter the ground stiffness. The 10kN/m trial is an outlier because the ground was so
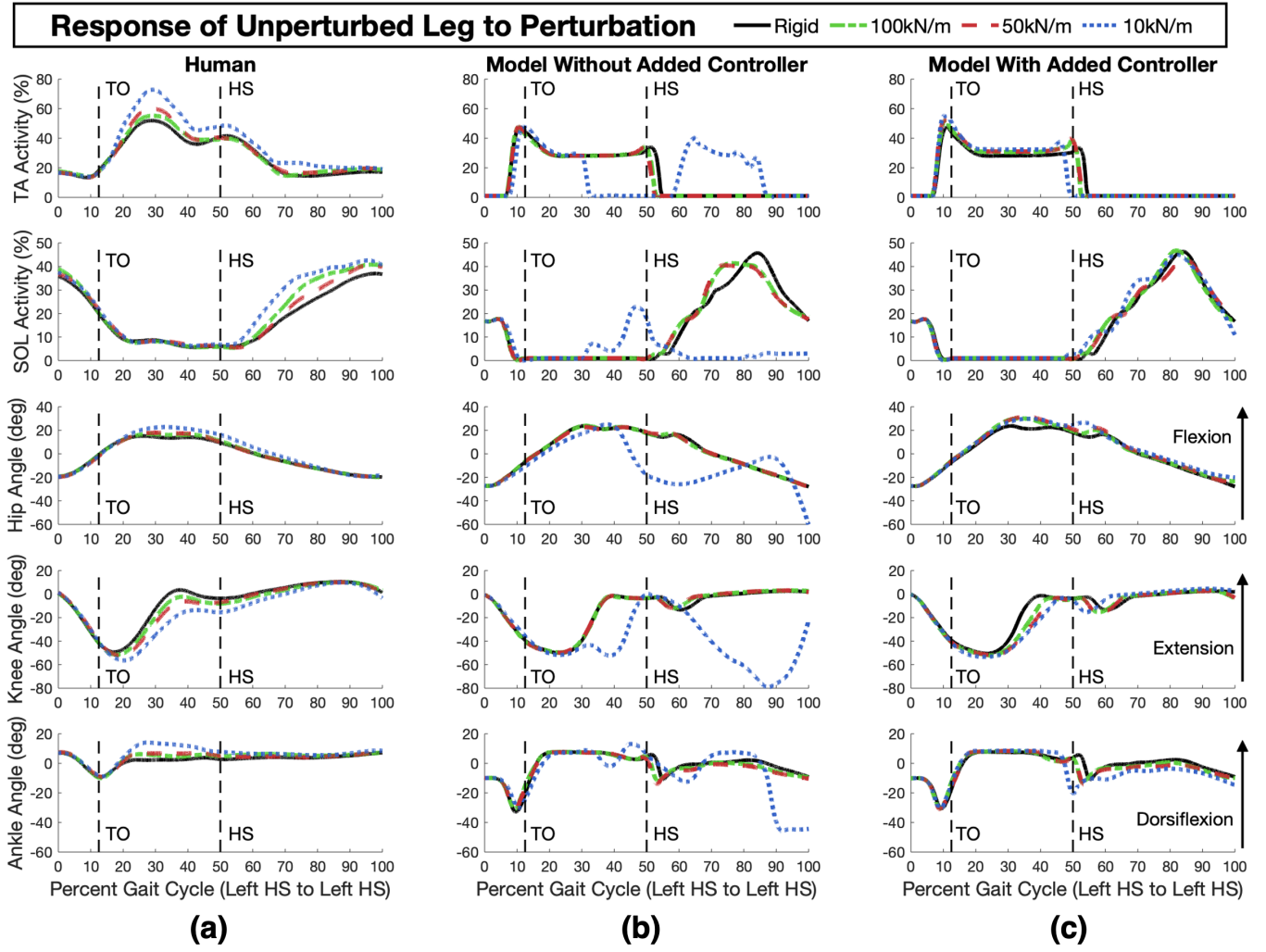
Fig. 4. Right side muscle activity and kinematic data after left side stiffness perturbation. Note that HS and TO are the heel strike and toe off of the unperturbed leg, respectively. (a) is the experimental human response. (b) is the model's response before any supraspinal changes were made. (c) is the model's response after the proposed supraspinal controller that modulates the target AoA and H2AS was added.

soft that the left foot of the model sank down far enough that the right foot experienced significant toe drag and fell immediately (Fig. 1). The other perturbation levels were not significant enough to cause the model to fall immediately, although it would fall within another step or two. Overall, the pre-modification model did not display adaptable behavior with the environment.

After modifying the model, significant improvements can be seen when comparing the final model response (Fig. 4c) with the human response (Fig. 4a). The model now displays very similar trends to the human data. In general, there is

separation between each of the different trials, signifying the model adapting to its surroundings. This can be seen best with the TA activity and the knee angle. The response of the model for different perturbation magnitudes are clearly distinguishable, and even deviate farther from the rigid trial as the magnitude of the perturbation increases. Also, none of the trials with the model display extreme outlier behavior as the 10kN/m response does in the pre-modification response of the model. This is because, post-modification, the model never experienced toe drag after a perturbation. Next, Table I shows a significant improvement in correlation coefficient

TABLE I
CORRELATION COEFFICIENT BETWEEN MODEL AND HUMAN DATA.

	TA		SOL		Hip		Knee		Ankle	
	Without Controller	With Controller	Without Controller	With Controller	Without Controller	With Controller	Without Controller	With Controller	Without Controller	With Controller
10 kN/m	-0.107	**0.454**	-0.199	**0.823**	0.660	**0.953**	-0.129	**0.959**	0.313	**0.508**
50 kN/m	0.540	0.537	0.667	0.734	0.938	0.936	0.964	0.926	0.438	0.411
100 kN/m	0.559	0.560	0.756	0.769	0.944	0.943	0.951	0.913	0.383	0.315

|	TA		SOL		Hip		Knee		Ankle	
	Without Controller	With Controller	Without Controller	With Controller	Without Controller	With Controller	Without Controller	With Controller	Without Controller	With Controller
10 kN/m	-0.276	**0.090**	-0.865	**0.267**	-0.439	**0.504**	-0.207	**0.686**	0.189	0.253
50 kN/m	0.269	0.276	-0.296	-0.391	-0.213	**0.762**	0.035	**0.705**	0.237	0.289
100 kN/m	0.278	0.299	0.004	-0.015	0.129	**0.715**	0.018	**0.573**	-0.098	-0.100
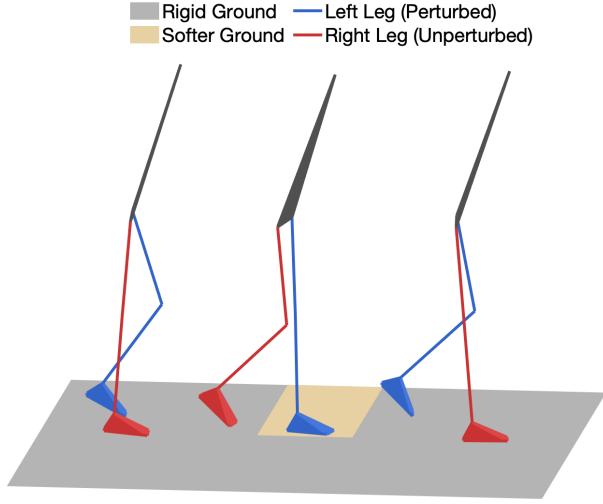
Fig. 5. Neuromuscular gait model, with added supraspinal controller, remaining balanced after a 10kN/m unilateral (left leg) stiffness perturbation (compare to Fig. 1).

values after adding the supraspinal controller to the 10kN/m trial. However, this method of comparison does not show significant change (positive or negative) for the 50kN/m or 100kN/m trials. It is for this reason that Table II was created. To reiterate, Table II shows the correlation between model and human data at 10kN/m, 50kN/m, and 100kN/m after their respective baseline (rigid trial) data has been subtracted from them. This table shows significant improvements in correlation for hip and knee kinematics for all three stiffness levels. While the same is not shown for the TA, SOL, and ankle, this was expected to a degree and will be further discussed in the Shortcomings section of the Discussion below. Last, after adding the high-level controller to select new target AoA and target H2AS values, the model stays upright and balances for multiple steps after all of the perturbation tests. The model can be seen in Fig. 5 staying balanced after the lowest stiffness perturbation of 10kN/m.

B. Angle of Attack & Hip to Ankle Span

After realizing the significant improvement that changing the target AoA and H2AS had on the model, we wanted to go back and confirm that the human subjects were also changing these same parameters. We decided to compare the AoA and H2AS in real time for the entire right swing phase after the perturbation for the model and human subjects on the VST [40]. For the sake of simplicity, we only compared two scenarios: no perturbation (rigid) and reduced stiffness

of 50kN/m. This comparison can be seen in Fig. 6, which shows that both the model and human subjects have a lower target AoA and H2AS when challenged with a low stiffness perturbation. This further validates altering the model's target AoA and H2AS to help it recover from a unilateral stiffness perturbation.

C. Response Equations

Aside from (3), two more relationships were uncovered. These equations are not directly used by the model, but were instead discovered based on how the model responded to different perturbation levels. The first of which relates the impulse error (ΔJ) to the stiffness of the perturbation (4).

$$\Delta J = \frac{c}{m} * e^{dK_p} \tag{4}$$

where $c = 1051.2\frac{kN*kg}{m}$, $d = -0.0117\frac{kN}{m}$, and K_p is the stiffness of the perturbation. The form of this equation was chosen first of all due to how well it fits the experimental data, with an R^2 value of 0.91 (see Fig. 7). The form was also chosen based on the behavior of the equation at $K_p = 0$ and as K_p approaches infinity. At $K_p = 0$, ΔJ takes on its maximum value, which corresponds to the maximum impulse error. This value can be thought of as the impulse felt on
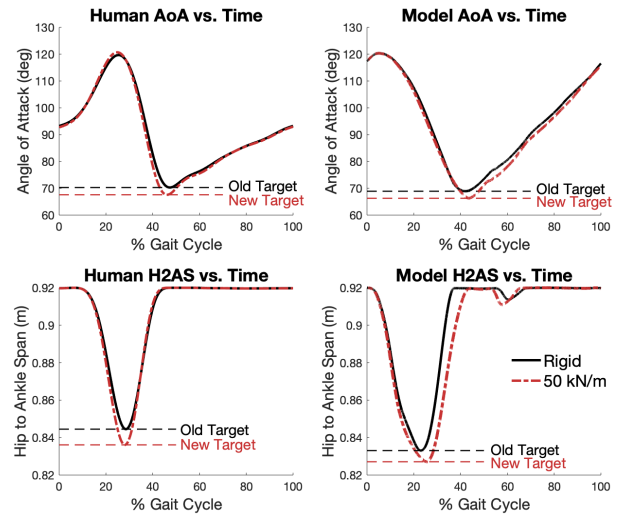

Fig. 6. Angle of attack and hip to angle span vs. time for both a human subject (left graphs) and the model (right graphs) displaying similar trends. This is in real time and the target values are marked on each respective graph. Referencing back to (2), "Old Target" corresponds to α or h and "New Target" corresponds to α_n or h_n. Only $50\frac{kN}{m}$ was displayed here for the sake of simplicity.

rigid ground, since there would be no ground reaction on a surface with a 0kN/m stiffness ($\Delta J = J_o$ since $J = 0$). As K_p approaches infinity, ΔJ approaches 0. This makes sense because as the ground stiffness increases beyond the 1000kN/m that was deemed rigid, ΔJ should continue to approach 0.

Finally, combining (3) and (4), (5) was derived. This shows the relationship between the gain value (G) used to modulate both the target AoA and H2AS and the stiffness of the perturbation. We believe this relationship could be useful in future medical applications and will be explained below in the Future Applications section of the Discussion.

$$G = \frac{p}{m^2} * e^{(dK_p)} + b \qquad (5)$$

where $p = -336.4kg^2$, $d = -0.0117\frac{kN}{m}$, and $b = 1$. These parameters were fit to experimental data with an R^2 value of 0.99.

V. Discussion

The results of this study suggest that the brain could be controlling interlimb coordination through target parameters such as target angle of attack (AoA) and target hip to ankle span (H2AS). This has the potential to shape future post-stroke rehabilitation methods using the VST. The rest of the discussion section will look further into the brain's involvement in interlimb coordination, point out shortcomings of the model used, and consider the future applications of these findings.

A. Supraspinal Involvement

This paper shows that by altering the target AoA, target H2AS and the relationship between TA activation and H2AS, we were able to produce muscle activity and kinematic data from the neuromuscular gait model that agrees with human subjects (see Fig. 4a and Fig. 4c). This is a significant contribution because it suggests a possible explanation as to how

Fig. 7.   Fitting (4) to experimental data.

human subjects are able to withstand and recover from unilateral stiffness perturbations using supraspinal mechanisms. Since previous studies have shown the brain's involvement in interlimb coordination after a unilateral stiffness perturbation, this study suggests that the brain may be controlling parameters such as AoA and H2AS when balancing after the perturbation [17], [18]. As stated previously, the target AoA and target H2AS were altered using the same gain value that was based on the impulse felt at heel strike. This impulse is clearly then related to the stiffness of the perturbation and quantifying these relationships might be useful for future model-based approaches.

To clarify, the model was not the inspiration to control target parameters that plan out the stride path. The model did however motivate looking specifically at the two variables (AoA and H2AS), as this is the method of stride planning it uses. The model is therefore imperative in developing the equations in this study.

B. Shortcomings

While the neuromuscular gait model used is extremely complex, it obviously does not exactly mimic human-like behavior. The discrepancy between the human and model responses could be a cause for questioning the significance of the results of this study, but we believe that the differences are minor enough that the results remain valid. The differences are discussed below.

First, the ankle kinematics from the model and human subjects (see Fig. 4a and Fig. 4c) simply do not match very well, and Tables I and II show that the ankle does not improve significantly outside of the 10kN/m trial. This is most likely due to the lack of toes on the model. The feet of the model use four contact points to interact with the ground, two at the heel of the foot and two at the ball. Because of the absence of toes, there is a lack of extra propulsion during toe off [41]. The model has to plantarflex more during toe off to generate sufficient thrust. Also, the model displays less dorsiflexion during mid to late swing. This is possibly also due to the model's lack of toes, resulting in a shorter foot length, and leading to a smaller required dorsiflexion angle to avoid toe drag. The issue with the ankle kinematics could also be due to the energy cost optimization this model uses to achieve locomotion [25]. The model tends to straighten the knee fairly early in the stance phase as this was found to be most energy efficient. This causes less dorsiflexion late in stance and explains why the model's ankle plantarflexes more towards 80% to 100% of the gait cycle [25].

Second, the tibialis anterior and soleus activity do not improve significantly in the 50kN/m and 100kN/m trials (see Tables I and II). This could first be due to these two stiffness levels not being severe enough to demand a significant change in muscle activity. It could also be due to the inherent shortcomings of the model. The baseline profile of the TA and SOL activity are not extremely similar. Peak muscle activation levels occur at different points in the gait cycle. Also, the model displays an "on/off" behavior at times that can be seen very well in the TA and SOL activity in Fig. 4c.
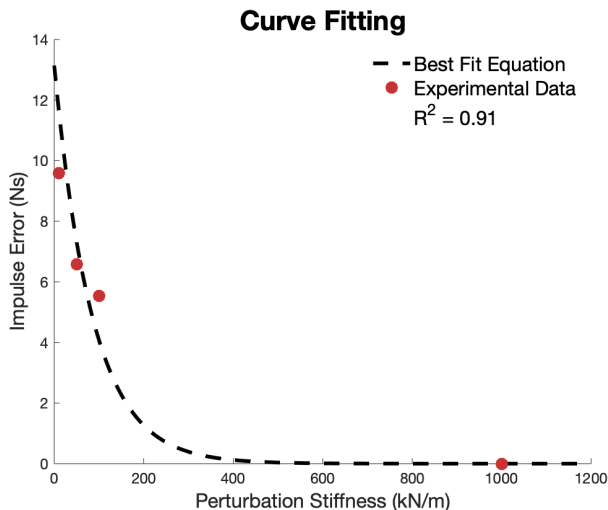
The model will make steep jumps from one level of muscle activity to another, even dropping to 0% for extended periods. This behavior is not seen in the human data (Fig.4a). Due to the difference in baseline human and model data, we were not expecting significant numerical improvements for the TA or SOL. Even the method of subtracting out the baseline data could not account for how different the model and human behave in terms of their muscle activity. However, we do not believe this is a major issue, as we were still able to visually distinguish between different trials and avoid any outliers. Additionally, significant improvements across all stiffness levels were made to the hip and knee kinematics, which are more important measures in achieving the desired functional outcomes of longer stride length and more ground clearance.

Finally, the model does not balance as well as a human. For VST experiments, human subjects that experienced unilateral stiffness perturbations were always able to remain upright and continue walking. For the model, this was not always the case. After a perturbation, the model would end up falling anywhere between one and six steps after the perturbation. This was mainly due to the fact that the added high-level controller only modulated the following contralateral step after the perturbation. The controller did not have a lasting effect that would have assisted in long-term balance recovery from the perturbation. Next, the model eventually falling could possibly be due to the model not being attached to a body weight support, assisting in remaining upright. Also, the lack of toes, as well as the simplification of the upper body to a rigid segment without arms, could have contributed to a lesser ability to balance. In human walking, both the toes and arms contribute to better balance, especially in terms of recovering from a perturbation [42]–[44]. For these reasons, the model remaining balanced and upright long after the perturbation was not the main concern of this study.

C. Future Applications

This study could aid in the future design of model-based stroke rehabilitation protocols. These protocols could be patient specific and perturb the subject in a systematic way that would lead to specific functional outcomes. Rearranging (5), we can acquire (6). This shows us what level of stiffness perturbation we would need in order to achieve a desired change in AoA and H2AS. In other words, this equation shows how we have control over a subject's AoA and H2AS by changing the magnitude of the controlled perturbation.

$$K_p = q \ln(r\, m^2 (G - b)) \tag{6}$$

where $q = -85.47 \frac{kN}{m}$, $r = -0.00297 kg^{-2}$, $b = 1$. Since this equation is simply a rearrangement of (5), it also has an R^2 value of 0.99.

Here is an example as to how this relationship could be useful: suppose we analyze the gait of a stroke patient (body mass of 80 kg) and conclude that their paretic leg is experiencing toe drag and taking smaller steps than the non-paretic leg. After a few calculations based off their

kinematics, we realize that their minimum AoA and H2AS need to be 4% smaller than what they currently are. Using (6), we can deduce that unilateral stiffness perturbations of 23 kN/m on the non-paretic leg would encourage the proper correction of the paretic leg's swing phase. Repetitive stiffness perturbations at that level could encourage the subject to walk with a decreased AoA and H2AS, and through practice, result in targeted rehabilitation protocols with specific functional outcomes.

Additionally, this study could help with controller design for robust bipedal robots, aiding in the ability of these robots to remain upright even after a significant unilateral perturbation caused by expected or unexpected walking surface changes.

VI. Conclusions

This paper suggests that after a unilateral stiffness perturbation, the brain may be controlling parameters such as target angle of attack and target hip to ankle span on the contralateral side to keep the body balanced. In this study, a neuromuscular gait model was compared to and tuned based on human subject experimental data. This model that was originally not able to withstand a unilateral stiffness perturbation was able to do so by changing the two target parameters (AoA and H2AS) based on the stiffness of the ground, using a new high-level controller. This relationship between perturbation level and the target parameters may be useful in the design of gait rehabilitation for stroke patients, hopefully correcting common post-stroke gait issues like unilateral shortened stride length and toe drag.

References

[1] P. W. Duncan, R. Zorowitz, B. Bates, J. Y. Choi, J. J. Glasberg, G. D. Graham, R. C. Katz, K. Lamberty, and D. Reker, "Management of Adult Stroke Rehabilitation Care," *Stroke*, vol. 36, no. 9, sep 2005.

[2] M. Grau-Pellicer, A. Chamarro-Lusar, J. Medina-Casanovas, and B. C. Serdà Ferrer, "Walking speed as a predictor of community mobility and quality of life after stroke," *Topics in Stroke Rehabilitation*, vol. 26, no. 5, pp. 349–358, jul 2019.

[3] P. Khanittanuphong and S. Tipchatyotin, "Correlation of the gait speed with the quality of life and the quality of life classified according to speed-based community ambulation in Thai stroke survivors," *NeuroRehabilitation*, vol. 41, no. 1, pp. 135–141, jan 2017.

[4] S. Li, G. E. Francisco, and P. Zhou, "Post-stroke hemiplegic gait: New perspective and insights," *Frontiers in Physiology*, vol. 9, no. AUG, p. 1021, aug 2018.

[5] E. J. Benjamin *et al.*, "Heart Disease and Stroke Statistics-2019 Update: A Report From the American Heart Association," *Circulation*, vol. 139, no. 10, pp. e56–e528, mar 2019.

[6] Y. R. S. Su, A. Veeravagu, and G. Grant, "Neuroplasticity after traumatic brain injury," in *Translational Research in Traumatic Brain Injury*. CRC Press, apr 2016, ch. 8, pp. 163–178.

[7] J. J. Daly and R. L. Ruff, "Construction of Efficacious Gait and Upper Limb Functional Interventions Based on Brain Plasticity Evidence and Model-Based Measures For Stroke Patients," *Discussion Paper TheScientificWorldJOURNAL*, vol. 7, pp. 2031–2045, 2007.

[8] S. Jezernik, G. Colombo, T. Keller, H. Frueh, and M. Morari, "Robotic Orthosis Lokomat: A Rehabilitation and Research Tool," *Neuromodulation*, vol. 6, no. 2, pp. 108–115, apr 2003.

[9] S. Hesse, D. Uhlenbrock, C. Werner, and A. Bardeleben, "A mechanized gait trainer for restoring gait in nonambulatory subjects," *Archives of Physical Medicine and Rehabilitation*, vol. 81, no. 9, pp. 1158–1161, sep 2000.

[10] J. F. Veneman, R. Kruidhof, E. E. Hekman, R. Ekkelenkamp, E. H. Van Asseldonk, and H. Van Der Kooij, "Design and evaluation of the LOPES exoskeleton robot for interactive gait rehabilitation," *IEEE Transactions on Neural Systems and Rehabilitation Engineering*, vol. 15, no. 3, pp. 379–386, sep 2007.

[11] A. Morbi, M. Ahmadi, and A. Nativ, "GaitEnable: An omnidirectional robotic system for gait rehabilitation," in *2012 IEEE International Conference on Mechatronics and Automation, ICMA 2012*, 2012, pp. 936–941.

[12] S. K. Banala, S. K. Agrawal, and J. P. Scholz, "Active Leg Exoskeleton (ALEX) for gait rehabilitation of motor-impaired patients," in *2007 IEEE 10th International Conference on Rehabilitation Robotics, ICORR'07*, 2007, pp. 401–407.

[13] M. Peshkin, D. A. Brown, J. J. Santos-Munné, A. Makhlin, E. Lewis, J. E. Colgate, J. Patton, and D. Schwandt, "KineAssist: A robotic overground gait and balance training device," in *Proceedings of the 2005 IEEE 9th International Conference on Rehabilitation Robotics*, vol. 2005, 2005, pp. 241–246.

[14] T. G. Hornby, D. D. Campbell, J. H. Kahn, T. Demott, J. L. Moore, and H. R. Roth, "Enhanced gait-related improvements after therapist-versus robotic-assisted locomotor training in subjects with chronic stroke: a randomized controlled study." *Stroke*, vol. 39, no. 6, pp. 1786–92, jun 2008.

[15] J. Hidler, D. Nichols, M. Pelliccio, K. Brady, D. D. Campbell, J. H. Kahn, and T. G. Hornby, "Multicenter randomized clinical trial evaluating the effectiveness of the Lokomat in subacute stroke," *Neurorehabilitation and Neural Repair*, vol. 23, no. 1, pp. 5–13, jan 2009.

[16] K. Arya and S. Pandian, "Interlimb neural coupling: Implications for poststroke hemiparesis," *Annals of physical and rehabilitation medicine*, vol. 57, 06 2014.

[17] J. Skidmore and P. Artemiadis, "Unilateral Floor Stiffness Perturbations Systematically Evoke Contralateral Leg Muscle Responses: A New Approach to Robot-Assisted Gait Therapy," *IEEE Transactions on Neural Systems and Rehabilitation Engineering*, vol. 24, no. 4, pp. 467–474, apr 2016.

[18] J. Skidmore and P. Artemiadis, "Unilateral walking surface stiffness perturbations evoke brain responses: Toward bilaterally informed robot-assisted gait rehabilitation," in *Proceedings - IEEE International Conference on Robotics and Automation*, vol. 2016-June. IEEE, may 2016, pp. 3698–3703.

[19] S. Grillner, "Control of Locomotion in Bipeds, Tetrapods, and Fish," in *Comprehensive Physiology*. Hoboken, NJ, USA: John Wiley & Sons, Inc., jan 2011, pp. 1179–1236.

[20] D. M. Armstrong, "Supraspinal contributions to the initiation and control of locomotion in the cat," *Progress in Neurobiology*, vol. 26, no. 4, pp. 273–361, jan 1986.

[21] S. Rossignol, R. Dubuc, and J. P. Gossard, "Dynamic sensorimotor interactions in locomotion," pp. 89–154, jan 2006.

[22] A. Barkan, J. Skidmore, and P. Artemiadis, "Variable Stiffness Treadmill (VST): A novel tool for the investigation of gait," in *Proceedings - IEEE International Conference on Robotics and Automation*. Institute of Electrical and Electronics Engineers Inc., sep 2014, pp. 2838–2843.

[23] J. Skidmore, A. Barkan, and P. Artemiadis, "Investigation of contralateral leg response to unilateral stiffness perturbations using a novel device," in *IEEE International Conference on Intelligent Robots and Systems*. Institute of Electrical and Electronics Engineers Inc., oct 2014, pp. 2081–2086.

[24] J. Skidmore, A. Barkan, and P. Artemiadis, "Variable Stiffness Treadmill (VST): System Development, Characterization, and Preliminary Experiments," *IEEE/ASME Transactions on Mechatronics*, vol. 20, no. 4, pp. 1717–1724, aug 2015.

[25] S. Song and H. Geyer, "A neural circuitry that emphasizes spinal feedback generates diverse behaviours of human locomotion," *Journal of Physiology*, vol. 593, no. 16, pp. 3493–3511, aug 2015.

[26] S. Song and H. Geyer, "Evaluation of a neuromechanical walking control model using disturbance experiments," *Frontiers in Computational Neuroscience*, vol. 11, p. 15, 2017.

[27] D. S. Reisman, H. J. Block, and A. J. Bastian, "Interlimb coordination during locomotion: What can be adapted and stored?" *Journal of Neurophysiology*, vol. 94, no. 4, pp. 2403–2415, oct 2005.

[28] S. M. Peterson and D. P. Ferris, "Differentiation in theta and beta electrocortical activity between visual and physical perturbations to walking and standing balance," *eNeuro*, vol. 5, no. 4, 2018.

[29] A. S. P. Sousa, A. Silva, R. Santos, F. Sousa, J. Manuel, and R. S. Tavares, "Interlimb Coordination During the Stance Phase of Gait in Subjects With Stroke Archives of Physical Medicine and Rehabilitation," *Archives of Physical Medicine and Rehabilitation*, vol. 94, pp. 2515–2522, 2013.

[30] H. Geyer and H. Herr, "A Muscle-reflex model that encodes principles of legged mechanics produces human walking dynamics and muscle activities," *IEEE Transactions on Neural Systems and Rehabilitation Engineering*, vol. 18, no. 3, pp. 263–273, jun 2010.

[31] P. E. Roos and J. B. Dingwell, "Influence of simulated neuromuscular noise on the dynamic stability and fall risk of a 3D dynamic walking model," *Journal of Biomechanics*, vol. 44, no. 8, pp. 1514–1520, may 2011.

[32] R. Baker, F. Leboeuf, J. Reay, and M. Sangeux, "The Conventional Gait Model - Success and Limitations," in *Handbook of Human Motion*. Springer International Publishing, 2017, pp. 1–19.

[33] A. Rajagopal, C. L. Dembia, M. S. DeMers, D. D. Delp, J. L. Hicks, and S. L. Delp, "Full-Body Musculoskeletal Model for Muscle-Driven Simulation of Human Gait," *IEEE Transactions on Biomedical Engineering*, vol. 63, no. 10, pp. 2068–2079, 2016.

[34] L. O. Christensen, N. Petersen, J. B. Andersen, T. Sinkjær, and J. B. Nielsen, "Evidence for transcortical reflex pathways in the lower limb of man," pp. 251–272, oct 2000.

[35] J. Skidmore and P. Artemiadis, "On the effect of walking surface stiffness on inter-limb coordination in human walking: Toward bilaterally informed robotic gait rehabilitation," *Journal of NeuroEngineering and Rehabilitation*, vol. 13, no. 1, mar 2016.

[36] S. Song and H. Geyer, "Generalization of a muscle-reflex control model to 3D walking," in *Proceedings of the Annual International Conference of the IEEE Engineering in Medicine and Biology Society, EMBS*, vol. 2013. Annu Int Conf IEEE Eng Med Biol Soc, 2013, pp. 7463–7466.

[37] R. Desai and H. Geyer, "Muscle-Reflex Control of Robust Swing Leg Placement," in *Proceedings - IEEE International Conference on Robotics and Automation*, 2013, pp. 2169–2174.

[38] N. Petersen, L. O. Christensen, H. Morita, T. Sinkjær, and J. Nielsen, "Evidence that a transcortical pathway contributes to stretch reflexes in the tibialis anterior muscle in man," *Journal of Physiology*, vol. 512, no. 1, pp. 267–276, oct 1998.

[39] J. Nielsen, N. Petersen, and B. Fedirchuk, "Evidence suggesting a transcortical pathway from cutaneous foot afferents to tibialis anterior motoneurones in man," *Journal of Physiology*, vol. 501, no. 2, pp. 473–484, 1997.

[40] M. Drolet, E. Q. Yumbla, B. Hobbs, and P. Artemiadis, "On the Effects of Visual Anticipation of Floor Compliance Changes on Human Gait: Towards Model-based Robot-Assisted Rehabilitation," in *IEEE International Conference on Robotics and Automation (ICRA)*. Institute of Electrical and Electronics Engineers (IEEE), sep 2020, pp. 9072–9078.

[41] F. Bojsen-Møller and L. Lamoreux, "Significance of free dorsiflexion of the toes in walking," *Acta Orthopaedica*, vol. 50, no. 4, pp. 471–479, 1979.

[42] M. Miyazaki, "Role and movement of the toes during walking," *Journal of the Japanese Orthopaedic Association*, vol. 67, no. 7, pp. 606–616, jul 1993.

[43] H. Takemura, A. Khiat, H. Iwama, J. Ueda, Y. Matsumoto, and T. Ogasawara, "Study of the toes role in human walk by toe elimination and pressure measurement system," in *Proceedings of the IEEE International Conference on Systems, Man and Cybernetics*, vol. 3, 2003, pp. 2569–2574.

[44] S. M. Bruijn, O. G. Meijer, P. J. Beek, and J. H. Van Dieën, "The effects of arm swing on human gait stability," *Journal of Experimental Biology*, vol. 213, no. 23, pp. 3945–3952, dec 2010.